POPULAR SUMMARY FOR THE ARTICLE

"Saharan Air and Atlantic tropical cyclone suppression from a global modeling perspective."

O. Reale, W. K. M. Lau, A. daSilva, K.-M. Kim.

being submitted to *Geophysical Research Letters*

During summer 2006, the NASA African Monsoon Multidisciplinary Analysis (NAMMA) organized a field campaign in Africa called Special Observation Period (SOP-3), in which scientists in the field were involved in a number of surface network and aircraft measurements. One of the scientific goals of the campaign was to understand the nature and causes for tropical cyclogenesis originating out of African Easterly Waves (AEWs, westward propagating atmospheric disturbances sometimes associated with precursors of hurricanes), and the role that the Saharan Air Layer (SAL, a hot and dry air layer advecting large amounts of dust) can play in the formation or suppression of tropical cyclones. During the NAMMA campaign a high-resolution global model, the NASA GEOS-5, was operationally run by the NASA Global Modeling and Assimilation Office (GMAO) in support to the mission. The daily GEOS-5 forecasts were found to be very useful by decision-making scientists in the field as an aid to discriminate between developing and non-developing AEWs and plan the flight tracks.

In the post-event analyses which were performed mostly by the Goddard Laboratory for Atmospheres, two events were highlighted: a non-developing AEW which appeared to have been suppressed by Saharan air, compared to a developing AEW which was the precursor of hurricane Helene. Both events were successfully predicted by the GEOS-5 during the real-time forecasts provided in support to the mission.

In this work it is found that very steep moisture gradients and a strong thermal dipole, with relatively warm air in the mid-troposphere and cool air below, are associated with SAL in both the GEOS-5 forecasts and the NCEP analyses, even at -great distance- from the Sahara.

The presence of these unusual thermodynamic features over the Atlantic Ocean, at several thousands of kilometers from the African coastline, is suggestive that SAL mixing is very minimal and that the model's capability of retaining the different properties of air masses during transport are important to represent effectively the role of dry air intrusions in the tropical circulation.

Saharan Air and Atlantic tropical cyclone suppression from a global modeling perspective.

O. Reale,[1,2] W. K. M. Lau,[1] A. daSilva,[3] K.-M. Kim[1,2]

This article investigates the role of the Saharan Air Layer (SAL) in two cases of non-developing and developing systems observed during the Special Observation Period (SOP-3) phase of the 2006 NASA African Monsoon Multidisciplinary Analyses (NAMMA). A high-resolution global model, the NASA GEOS-5 was operationally run by the NASA Global Modeling and Assimilation Office (GMAO) in support to the NAMMA field campaign, which included surface network and aircraft measurements. One of the scientific goals of the campaign was to understand the nature and causes for tropical cyclogenesis out of African Easterly Waves (AEWs). The daily GEOS-5 forecasts were found to be very useful by decision-making scientists in the field as an aid to discriminate between developing and non-developing AEWs and plan the flight tracks. In the post-event analyses of a non-developing system which appeared to have been suppressed by SAL, it has been found that very steep moisture gradients and a strong thermal dipole are associated with SAL in both the GEOS-5 forecasts and the NCEP analyses, even at great distance from the Sahara. This is suggestive that SAL mixing is very minimal and that the model's capability of retaining the different properties of air masses during transport is important to represent effectively the role of dry air intrusions in the tropical circulation.

1. Introduction

African Easterly Waves (AEWs) have been recognized as prominent weather-producing events of northern tropical Africa [e.g Burpee, 1974; Asnani, 2005] and have been extensively studied from observational and modeling perspectives [e.g Hsieh and Cook, 2005; Kiladis et al., 2006].

However, the development of AEWs into tropical depressions remains one of the most challenging problem in the prediction and modeling of Atlantic tropical cyclones. The Saharan Air Layer (SAL), a layer of hot dry air rich in dust and produced over the Saharan desert, has been investigated with the aid of Geostationary Operational Environmental Satellite (GOES) by Dunion and Velden [2004] and recognized as a possible, important mechanism

[1]NASA Goddard Space Flight Center, Laboratory for Atmospheres, Greenbelt, Maryland, USA.

[2]University of Maryland, Baltimore County, Baltimore, Maryland, USA.

[3]NASA Goddard Space Flight Center, Global Modeling and Assimilation Office, Maryland, USA.

0094-8276/07/$5.00

concurring to tropical cyclone suppression.

The general problem of tropical cyclogenesis has always been considered from either strictly observational or high-resolution mesoscale points of view, because the lower resolution of global models is deemed to be inadequate to trigger spontaneous cyclogenesis. However, in recent years a number of global models have reached the resolution of 10-40 km and have started to display some tropical cyclogenesis capability [e.g Atlas et al., 2005; Shen et al., 2006].

The organization of several convective centers into a rotating system still requires cloud-resolving models and can not be reproduced by real-time global numerical weather prediction models. However, the process of cyclogenesis or cyclogenesis suppression can be studied from different perspectives, and global models do have the advantage of better capturing the large-scale forcings involved. In particular, a global model can be used to investigate the role of SAL not only on the wave scale, but also from the point of view of the large-scale transport from its source region, and can therefore represent the possible modification of thermodynamical properties, as the waves propagate over thousands of kilometers. At the same time, sufficiently high resolution is needed to unveil some of the SAL kinematic features, such as the increasingly narrow structure of the dry air filaments being intruded in a tropical circulation, and the sharpness of the boundaries between Saharan and non-Saharan air.

2. The Model

In this work, the effect of Sahara air is investigated using a high-resolution global atmospheric model, the NASA GEOS-5, documented in Bosilovich et al. [2006]. The GEOS-5 shares the same dynamical core [Lin, 2004] with the so-called NASA finite-volume General Circulation Model (fvGCM) which has demonstrated remarkable capabilities in hurricane forecasting [Atlas et al., 2005; Shen et al., 2006]. The GEOS-5 however contains a new physics developed predominantly by the Global Modeling and Assimilation Office (GMAO), which is substantially different from the previous fvGCM. The version used during NAMMA was run at a horizontal resolution of $0.25^o \times 0.33^o$ with 72 vertical levels.

3. MAP06 and NAMMA

Over the past ten years, the NASA Global Modeling and Assimilation Office, continuing the work previously done in the Data Assimilation Office, has been increasing the resolution of its global model and performing real-time forecasts. During the Atlantic tropical seasons of 2005, 2006 and 2007 the current high resolution version of the model was put to a severe test by providing real-time forecasts that could be compared to operational state-of-the-art models. GEOS-5 was made available to the operational team in Africa, as an auxiliary decision support tool in the SOP-3 phase of the NAMMA campaign. The model performed well and the forecasts were found beneficial by the team on the field. After-event analysis has revealed some interesting aspects of the cyclogenetic process as perceived by the model, and on the impact of SAL in the development or suppression of storms.

4. Analysis

In this work we focus on two interesting events observed during the SOP-3 NAMMA campaign: one nondeveloping and one developing wave, appearing quite similar in terms of intensity, vertical shear and other dynamical forcings, and we investigate their different evolution and the different properties of the corresponding SAL intrusions. Figure 1 shows a Hovmøller of 850hPa relative vorticity and total precipitable water from the operational NCEP analyses to emphasize AEWs during the first 15 days of the SOP-3, covering the second half of August. The strongest wave of the period appears in the diagram on 23 August at about $5^o W$ and undergoes transition on the following day (hereafter W1). An evident sharp strip of dry air with the same propagation speed and amplitude of the wave, clearly associated with a Saharan Air outbreak, can be seen.

In Figure 2, 700 hPa specific humidity and 850 hPa flow are shown together to emphasize the interaction between two different levels at the initial time (00z 26 August, from NCEP analyses) and across 3 times of the forecast (24, 48 and 72 hour forecast, corresponding to verification times of 00z 27, 28 and 29 August respectively). The 700hPa level is at the lower part of the SAL, whereas 850 corresponds approximately to the top of the moist lower level and emphasizes the low-level circulation. Flows at 700 and 850 hPa are substantially different except around the storm center, where a vertically aligned circulation is present from the surface up to almost 500 hPa. Based upon these forecasts, it was correctly suggested to the NAMMA forecasting team on the field that W1 would become a nondeveloping wave in spite of its apparent strength. The team obviously had many other forecasting tools available but the information provided by the GEOS-5 was correct. Following the path of the dry air at 700 hPa it can be seen that as soon as dry air is advected on the top of the 850 hPa circulation center, the rotating system becomes first elongated and then rapidly evolves into an open wave. This is even more evident while analyzing intermediate timesteps (not shown).

In Figure 3, a zonal vertical cross-section of specific humidity at $20^o N$ is extracted from the GEOS-5 24-hour forecast, right across the center of the same circulation which can still be seen in Figure 2 at 00z 27 August. An intriguing feature, namely a sharply defined 'corridor' of extremely dry air can be seen down to 800 hPa. Remarkable moisture gradients are present on both sides. From the temperature anomaly (obtained by subtracting the zonal mean between $80^o W$ and 0^o), a very well-defined thermal dipole, stronger than any other anomaly in the range of longitudes selected, can be seen in perfect correspondence to the dry tongue. In particular, a warm anomaly spans between 800hPa and 400hPa, and a cool anomaly between 825 hPa and the surface. In other words, since the cross-section cuts across the SAL intrusion, it appears that temperature, in the core of the SAL, is approximately $3^o C$ warmer than the surroundings at the same latitude, in partial agreement with Dunion and Velden, [2004]. The new aspect of this analysis is however that a *negative* value also detected in the moist low-level layer at the base of the column.

In Figure 4, the same figure is extracted from the full-resolution NCEP operational analyses in model levels. 0.5 corresponds roughly to 500 hPa. The Figure confirms the thermal structure depicted in the GEOS-5 24-hour forecast. Despite small scale differences, the NCEP analyses confirm the presence of a very well-defined dry intrusion at about $35^o - 40^o W$. Most remarkable is the presence of the same dipole thermal anomaly seen in Figure 3.

A positive value reaching 4^oC in the mid-troposphere, and a corresponding cool anomaly down to -4^oC in the low moist layer. The anomalies are obtained, as in Figure 3, by simply subtracting the $80^oW - 0^o$ mean.

In contrast to Fig 1, the Hovmøller computed for September (Figure s1) shows a powerful wave towards the end of SOP-3 (hereafter W2) associated to some Saharan Air: however, the magnitude of the SAL is not comparable with the case of W1.

In Figure 5, the same zonal cross-section is produced across the center of the system W2, which is a precursor of Helene: the vertically aligned vorticity column at about 33^oW is the analyzed signature of the Tropical Storm, named at 00z 14 September 2006 [Brown, 2006]. A weak positive temperature anomaly at about $40-45^oW$ in the lower midtroposphere is associated with the same Saharan air outbreak which can be detected in the Hovmøller in Figure S1. However, two prominent differences can be seen with respect to the non-developing W1 in Figures 3 and 4: there is no cool anomaly in the lowest levels, and the dry air appears more diluted with less sharp horizontal gradients.

The real-time GEOS-5 tropical cyclogenesis forecast for Helene was correct. In Figure S2, the 850 hPa circulation shows a clearly defined vortex (at about $24-25^oW$ and $10-12^oN$ in the initial conditions) progressing westward and then recurving northwestward, being entangled in corresponding high levels of 700 hPa moisture. Based upon this and other information, subjective forecasts on the field considered the possibility of that system to be a developing one, and one flight was successfully planned across it.

Post-event model analysis suggests that since vertical shear and all other environmental conditions were very favorable in both W1 and W2 case (not shown), but only the latter underwent development becoming Helene, the only difference appears to be the intensity of the Saharan Air intrusion. In the model, the temperature dipole associated to the SAL could be followed at each timestep and can be considered a possible cause of suppression. In the precursor of Helene, the low-level negative anomaly was minimal or absent.

While the positive anomaly can be simply attributed to the signature of warm air originated over the Sahara, the cool anomaly in the lower levels does not have any plausible explanation relying on transport only. There is no source of localized cooler temperatures at that latitude, away from landmass and in a very homogeneous marine tropical environment. At this time, albeit speculative, a possible explanation is that the low-level cool temperatures are an indirect evidence of dust amount. The thermal effect of Saharan mineral dust is a net reduction of downwave shortwave radiation in the near-surface levels, and a heating in the lower midtroposphere, corresponding to the core of the SAL. It appears that the high-resolution NCEP, unlike lower resolution analyses, can represent this thermal structure and that the GEOS-5 model initialized by the NCEP analyses could retain it for 24-72 hours advecting it into the circulation and producing a realistic cyclone dissipation.

In the case of the GEOS-5 forecast, the nature of the finite-volume dynamics [Lin, 2004] is such that is a particularly suitable tool to generally maintain sharp gradients by minimizing unrealistic diffusion processes. The finite-volume dynamics has been shown to be very efficient in the midlatitudes where localized temperature gradients associated with sharp fronts can be very realistically simulated and maintained. This work documents that the same skill can be very useful also in the tropics when dealing with Saharan Air.

5. Concluding Remarks

This work documents the contribution of the NASA Global Modeling and Assimilation Office in support to the SOP-3 phase of the NAMMA campaign. From the 30 5-day forecasts, one prominent case is extracted, a very strong non-developing wave, and is compared with the wave that becomes the precursor of Hurricane Helene. GEOS-5 forecasts and NCEP full-resolution analyses document the presence of a strong temperature dipole (cooler than the environment below 800hPa, and warmer from 800 to 500hPa) associated with the Saharan air intrusion. This dipole is advected into the circulation of the wave, suppressing further development. No such dipole is found for the Saharan air intruded in the Helene's precursor. The lower tropospheric cooling associated with the strong Saharan air outbreak is suggestive that the high resolution global models and analyses can capture part of the thermal effect consequent to downward shortwave reduction caused by large amounts of Saharan dust. An interactive dust aerosol component, including its direct radiative effects, is being employed within GEOS-5 to further assess and quantify the thermal effects of dust on tropical cyclogenesis and will be used for a future study.

Acknowledgments. Authors acknowledge support from Ramesh Kakar through the NAMMA Project. Thanks are also due to Michele Rienecker for access to the GEOS-5 forecasts.

References

Asnani, G. C. (2005), *Tropical Meteorology.* Publisher: Indian Institute of Tropical Meteorology, Pashan, Pune-411008, India. 3 vols.

Atlas, R., O. Reale, B.-W. Shen, S.-J. Lin, J.-D. Chern, W. Putman, T. Lee, K.-S. Yeh, M. Bosilovich, and J. Radakovich (2005), Hurricane forecasting with the high-resolution NASA finite-volume general circulation model. *Geophysical Research Letters,* **32,** L03807, doi:10.1029/2004GL021513.

Bosilovich, M. G., S.D. Schubert, M. Rienecker, R. Todling, M. Suarez, J. Bacmeister, R. Gelaro, G.-K. Kim, I. Stajner, and J. Chen, (2006), NASA's Modern Era Retrospective-analysis for Research and Applications. U.S. CLIVAR Variations, 4 (2), 5-8.

Brown, D. P., (2006), Tropical Cyclone Report. Hurricane Helene (AL082006). 12-24 September 2006. Available online at

`http://www.nhc.noaa.gov/pdf/TCR-AL082006_Helene.pdf`

Burpee, R. W. (1974), Characteristics of north African Easterly waves during the summers of 1968 and 1969. J. Atmos. Sci, **31,** 1556-1570.

Dunion, J., and C. S. Velden, (2004), The impact of the Saharan Air Layer on Atlantic Tropical Cyclone activity. *Bull. Am. Meteorol. Soc., 85, 353-365.*

Hsieh, J.-S., and K. Cook (2005), Generation of African Easterly Wave disturbances: Relationship to the African Easterly Jet. *Mon. Wea. Rev.* **133,** 1311-1327.

Kiladis, G. N., C. D. Thorncroft, and N. M. J. Hall (2006), Three-Dimensional Structure and Dynamics of African Easterly Waves. Part I:Observations, *J. Atmos. Sci.,* **63,** 2212-2230.

Lin, S.-J., 2004: A 'vertically lagrangian' finite-volume dynamical core for global models, *Mon. Wea. Rev., 132,* 2293-2307.

Shen, B.-W., R. Atlas, O. Reale, S.-J. Lin, J.-D. Chern, J. Chang, C. Henze, and J.-L. Li (2006), Hurricane forecasts with a global mesoscale-resolving model: Preliminary results with Hurricane Katrina (2005). *Geophysical Research Letters,* 33, L13813, doi:10.1029/2006GL026143.

O. Reale, Laboratory for Atmospheres, Code 613, NASA Goddard Space Flight Center, Greenbelt, MD 20771, USA. (Oreste.Reale-1@nasa.gov)

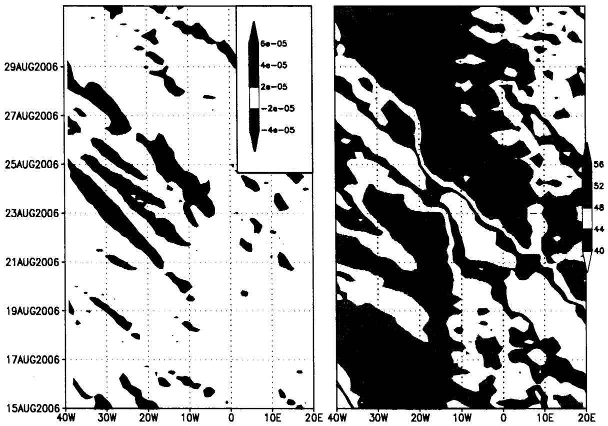

Figure 1. Hovmøller of 850 hPa relative vorticity (s^{-1}, left panel) and total precipitable water (right panel) from the NCEP operational analyses, latitudinally averaged ($10^o - 18^o N$), covering the period from 16 to 31 August. Data on pressure levels interpolated on a 1^o resolution grid. No significant difference from the original data in sigma levels (not shown).

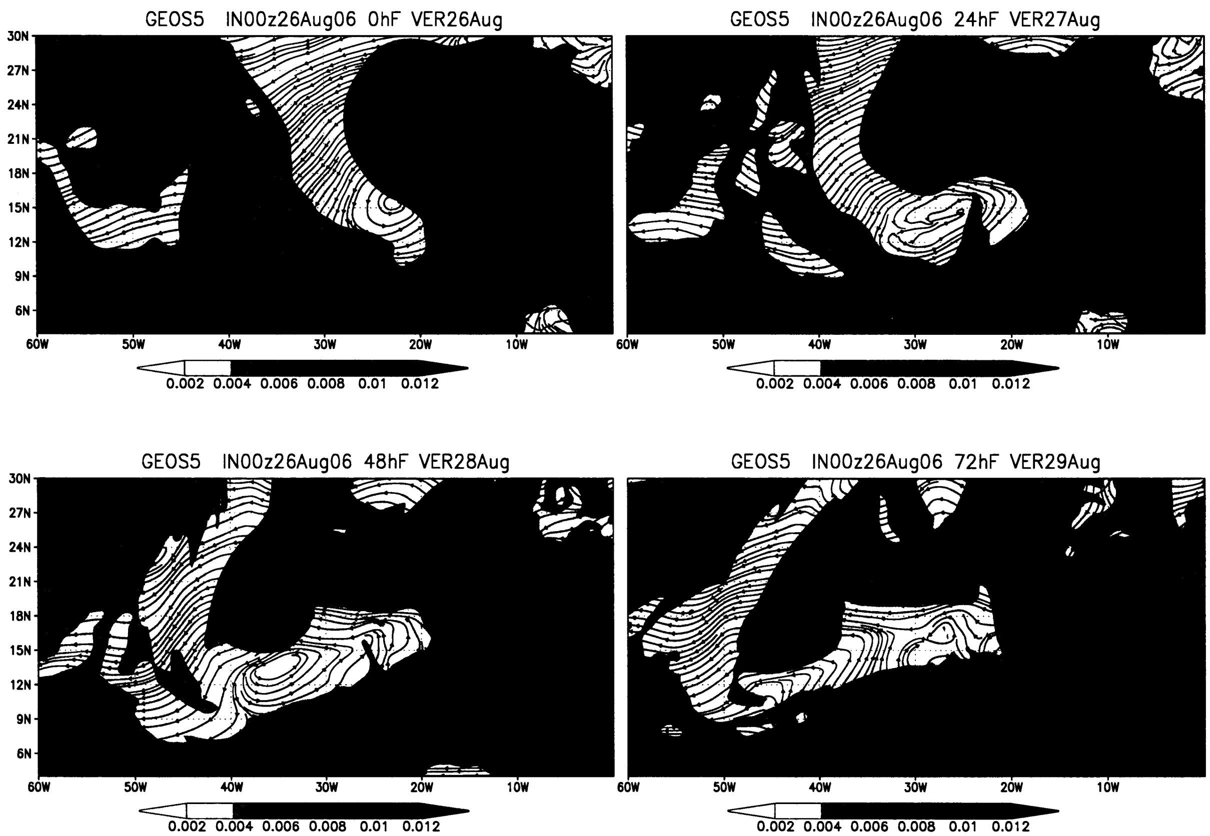

Figure 2. GEOS-5: 700 hPa specific humidity ($KgKg^{-1}$) and 850 hPa wind (streamlines) in the NCEP-derived initial conditions (upper left) for 00z 26 August, and relative to the 24, 48 and 72 hour forecasts for 00z 26, 27 and 28 August.

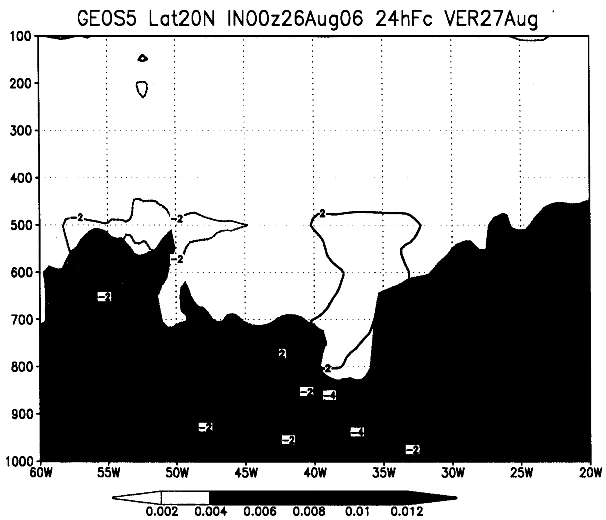

Figure 3. GEOS-5: zonal vertical cross-section of specific humidity ($KgKg^{-1}$, shaded) and temperature anomaly (^oC, contour, subtracting the zonal mean between 80^oW and 0^o) at 20^oN for 27 August, 24 hour forecast initialized at 00z 26 August.

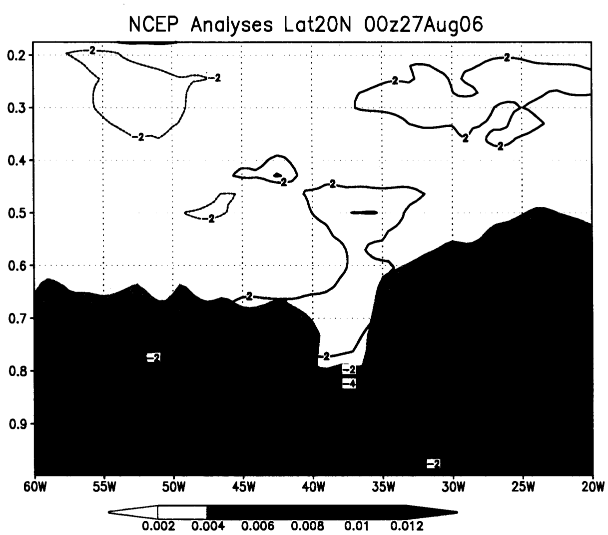

Figure 4. NCEP full-resolution analyses in model levels: zonal vertical cross-section of specific humidity ($KgKg^{-1}$, shaded) and temperature anomaly (^oC, contour, subtracting the zonal mean between 80^oW and 0^o) at 20^oN for 00z 27 August. The vertical dimension is only approximately comparable with Figure 3 since the spacing between model levels and pressure levels is different.

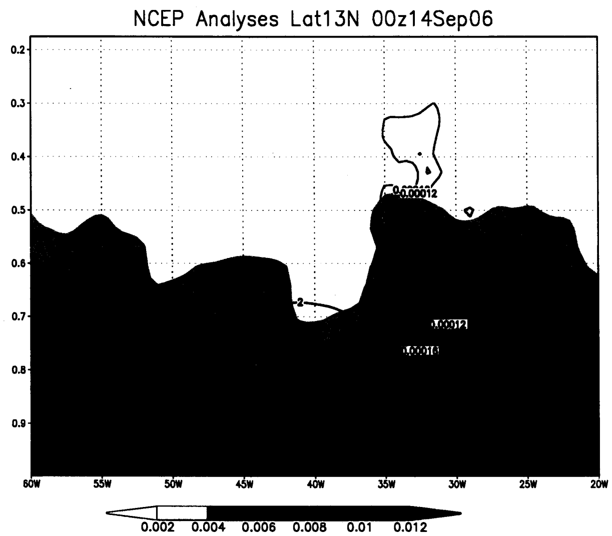

Figure 5. NCEP full-resolution analyses in model levels: zonal vertical cross-section of specific humidity ($KgKg^{-1}$, shaded), temperature anomaly (^oC, contour, subtracting the zonal mean between 80^oW and 0^o) and relative vorticity (s^{-1}, contour) at 13^oN for 00z 14 Sep, across the center of the newly named Tropical Storm Helene.

Auxiliary Material

Two additional figures are provided to allow a comparison with
Fig. 1 and Fig. 5 in the paper.

grl_fs01.eps
Caption:
Hovmoller of 850 hPa relative vorticity (left panel)
and total precipitable water (right panel) from the NCEP operational
analyses, latitudinally averaged (10-18N),
covering the period from 1 to 15 September.
Data on pressure levels interpolated on a 1 degree resolution grid.
No significant difference from the original data in
sigma levels (not shown).

grl_fs02.eps
Caption:
GEOS-5: 700 hPa specific humidity (Kg/Kg) and
850 hPa wind (streamlines) in the NCEP-derived
initial conditions (upper left) for 00z 13 September, and
relative to the 24, 48 and 72 hour forecasts for
00z 14, 15 and 16 September.

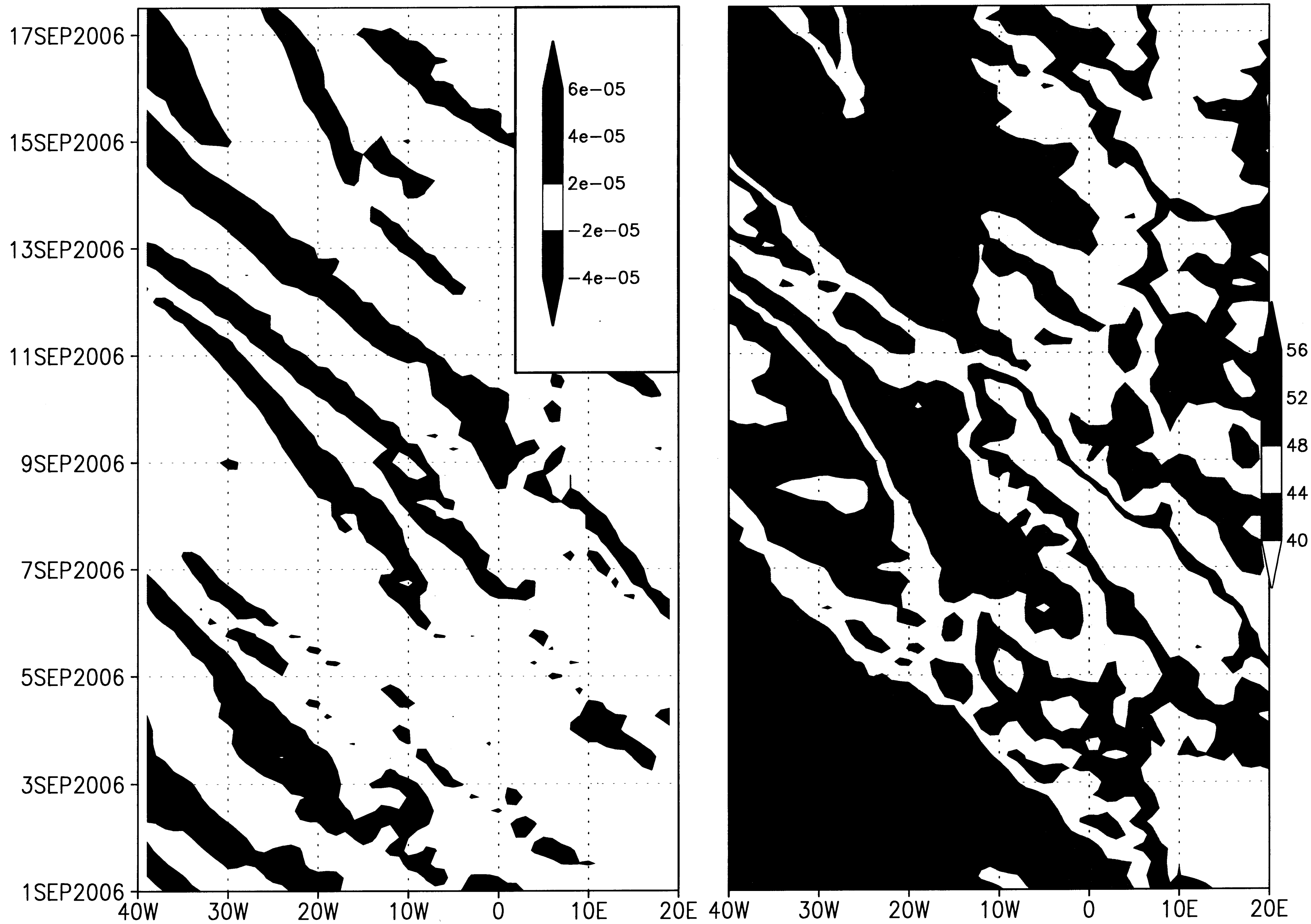

17SEP2006
15SEP2006
13SEP2006
11SEP2006
9SEP2006
7SEP2006
5SEP2006
3SEP2006
1SEP2006
40W
30W
20W
10W
0
10E
20E
6e−05
4e−05
2e−05
−2e−05
−4e−05
56
52
48
44
40

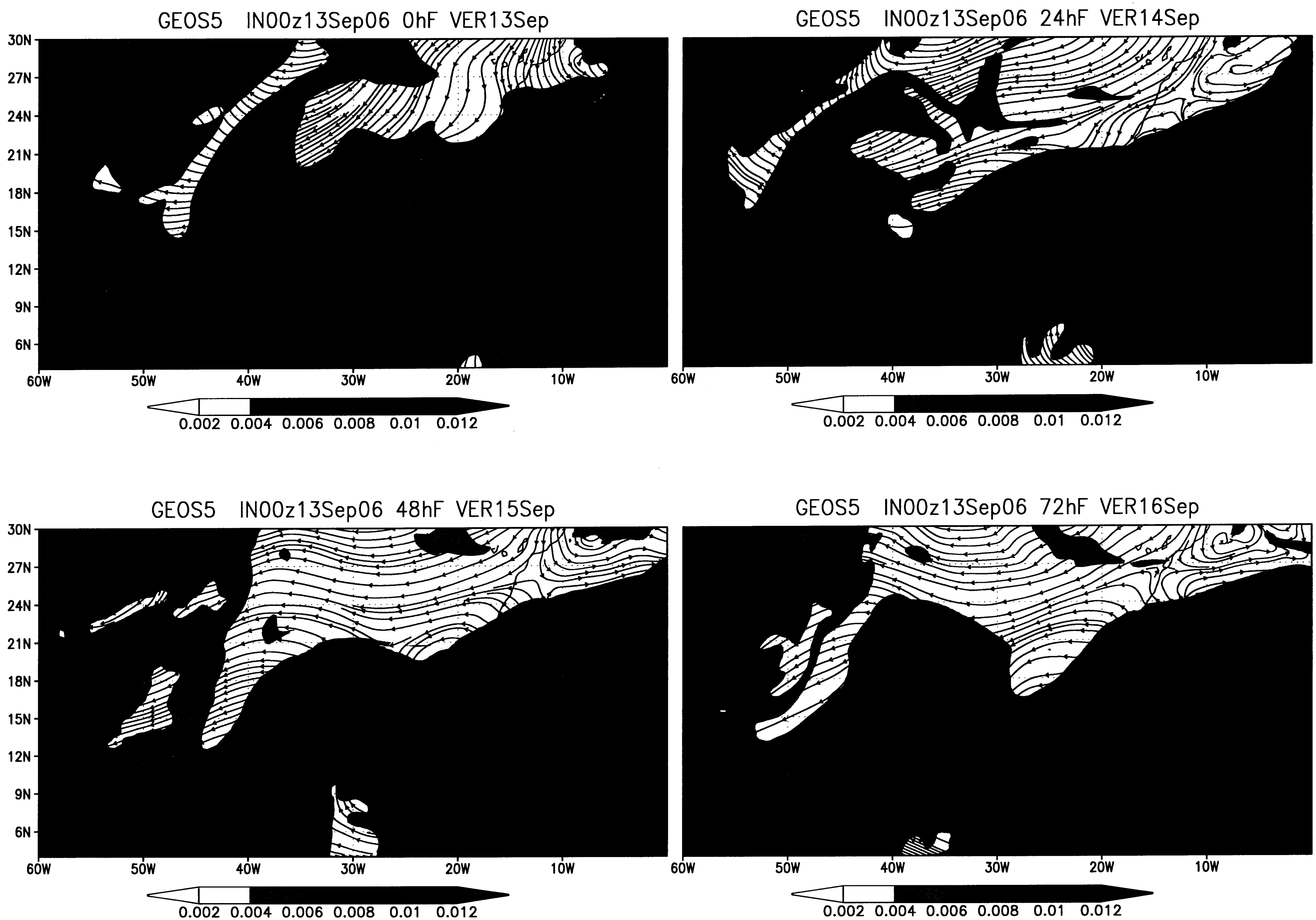
GEOS5 IN00z13Sep06 0hF VER13Sep
GEOS5 IN00z13Sep06 24hF VER14Sep
GEOS5 IN00z13Sep06 48hF VER15Sep
GEOS5 IN00z13Sep06 72hF VER16Sep
30N 27N 24N 21N 18N 15N 12N 9N 6N
60W 50W 40W 30W 20W 10W
0.002 0.004 0.006 0.008 0.01 0.012